

Electron-phonon interaction and electronic correlations in transport through electrostatically and tunnel coupled quantum dots

Damian Krychowski^{1,*} and Stanisław Lipiński^{1,†}

¹*Institute of Molecular Physics, Polish Academy of Sciences, Smoluchowskiego 17, 60-179 Poznań, Poland*

(Dated: November 20, 2023)

We investigate two equivalent capacitively and tunnel coupled quantum dots, each coupled to its own pair of leads. Local Holstein type electron-phonon coupling at the dots is assumed. To study many-body effects we use the finite-U mean-field slave boson approach. For vanishing interdot interaction, weak e-ph coupling and finite tunneling, molecular orbital spin Kondo effects occur for single electron or single hole occupations. Phonons influence both correlations and tunneling and additionally they shift the energies of the dots. Depending on the dot energies and the strength of electron-phonon coupling, the system is occupied by a different number of electrons that effectively interact with each other repulsively or attractively leading to a number of different ground states of DQD. Among them are Kondo-like states with spin, orbital or charge correlations resulting from polaron cotunneling processes and states with magnetic intersite correlations.

I. INTRODUCTION

In double quantum dots (DQD) both spin and orbital degrees of freedom are relevant, which leads to creating various correlated states. Multi-dot devices allow studying these phenomena in more detail than in bulk systems, because at nano scale it is possible to tune the couplings at will. The interest in quantum dot arrangements stems also from their potential applications for spintronics and quantum computation [1, 2]. Depending on DQD geometry (series or parallel coupled) continuous or discontinuous transitions between different ground states have been predicted [3]. Most of the papers concern the dots connected in series, but recently, it has been realized that parallel double quantum dots are much more experimentally suitable than dots in series for studying spin entangled states composed of coherent Kondo resonances [4]. Many publications, both theoretical and experimental have been already devoted to this subject (e.g. [5–10]). Recently nano-electromechanical systems (NEMS) have attracted much interest, because they integrate electrical and mechanical functionalities [11, 12]. Particularly attractive in this respect are molecular systems due to their softness. Among the hot topics studied is the impact of electron - phonon (e-ph) coupling on electron correlations [13–19]. A very useful method of experimental study of these subtle effects are the conductance measurements e.g. observation of Kondo phonon satellite peaks [20]. Similar phenomena have been also reported in the rigid structures of semiconductor QDs embedded in a freestanding GaAs/AlGaAs membrane [21]. Advanced nanotechnology has been able to provide a good morphology manipulation of semiconductor QDs such as size, shape strain distribution, and inhomogeneities, which determine the effective e-ph interaction [22]. Similar research opportunities for studying impact of phonons on

transport for different phonon frequencies and different coupling constants exist in carbon nanotubes, since these quantities depend on the microscopic details of CNT, such as its chirality and radius [23, 24].

In this paper, we investigate the role of e-ph interaction in the occurrence of various highly correlated DQD behaviors and the reflection of these phenomena in transport properties. We examine impact of phonons on the competition between Kondo phases and local singlet phases in spin and charge degrees of freedom. If the vibration energy exceeds the hybridization energy between dot and electrode electrons (antiadiabatic limit), then strong local Holstein e-ph coupling drives the system towards polaron states localized at the single dot. E-ph coupling introduces attractive interdot interaction and suppresses tunneling. For intermediate e-ph coupling, when phonon induced attractive interaction is smaller than Coulomb repulsion and tunneling to the leads is not completely suppressed by phonons. For weak and intermediate interdot tunneling and weak e-ph coupling single site spin Kondo effects occur for odd occupancies of DQD and they transform into molecular spin Kondo states for stronger interactions with phonons. For still higher values of e-ph coupling transitions into higher occupancies result and Kondo resonances are destroyed. When two electrons reside on the dots and e-ph coupling is weak local spin singlet forms. For stronger interactions with phonons subsequent transitions into different Kondo states occur. For the electrostatically decoupled dots successive states appear with increasing e-ph interactions: orbital Kondo, two-site Kondo and charge-orbital Kondo states. The latter occurs when phonon induced attraction exceeds Coulomb repulsion. For electrostatically coupled dots the similar sequence of states for increasing e-ph coupling in double occupancy is: orbital Kondo, two-site Kondo state and isospin correlated Kondo state.

* krychowski@ifmpan.poznan.pl

† lipinski@ifmpan.poznan.pl

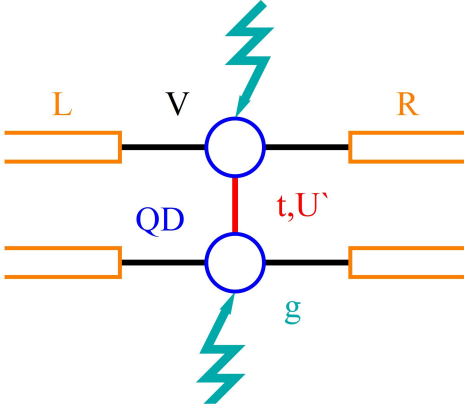


Figure 1. (Color online) Schematic of the parallel double-quantum dot setup attached to separate leads with interorbital Coulomb interaction (U') and tunnel coupling between the dots (t). Hopping parameter to the electrodes is denoted by V . Electrons on the dots are coupled to local phonons with e-ph strength g (wavy lines).

II. MODEL AND FORMALISM

We consider two equivalent single-level coupled quantum dots, each coupled to its own pair of leads (Fig.1). The local electron densities at the dots are coupled to local vibrations. The system is modeled by Anderson-Holstein two-impurity Hamiltonian:

$$H = H^e + H^{ph} + H^{e-ph} \quad (1)$$

where

$$H^e = \sum_{ls} E_d n_{ls} + \sum_s t (d_{1s}^\dagger d_{2s} + h.c.) + U \sum_l n_{l\uparrow} n_{l\downarrow} + U' \sum_{ss'} n_{1s} n_{2s'} + \sum_{k\alpha ls} E_{k\alpha ls} n_{k\alpha ls} + \sum_{k\alpha ls} V (c_{k\alpha ls}^\dagger d_{ls} + h.c.)$$

The first term represents site energies of the dots, the next tunnel coupling between the dots (t), the terms parameterized by U and U' describe intra- and interdot Coulomb interactions respectively and the last two terms describe electrons in the electrodes and their tunneling to the dots (V). We assume the coupling strength to the electrodes with the rectangular density of states $1/2D$ for $|E| < D$ is $\Gamma = \pi V^2/2D$, with D denoting the electron bandwidth of electrodes.

The phonon and e-ph coupling terms are given by:

$$H^{ph} + H^{e-ph} = \sum_l \omega_0 a_l^\dagger a_l + \sum_l g \cdot n_l (a_l^\dagger + a_l) \quad (2)$$

The first term describes local Einstein phonons of energy ω_0 and the second their linear coupling to electrons at the dots. We assume non-adiabatic regime ($\omega_0/\Gamma > 1$) and strong electron-phonon coupling limit, in which case one can eliminate linear e-ph coupling terms by the Lang-Firsov unitary transformation (L-

F) [25] $\bar{H} = e^{i(S_1+S_2)} H e^{-i(S_1+S_2)}$, defined by generators $S_l = (g/\omega_0) n_l (a_l^\dagger - a_l)$, ($n_l = \sum_s n_{ls}$). L-F approach is exact if $V = 0$ or $g \rightarrow +\infty$. L-F transformation shifts the dots to the new equilibrium positions and in general changes the phonon vacuum. The new fermion (polaron) operators are $\bar{d}_{ls} = d_{ls} X_l$ and $\bar{d}_{ls}^\dagger = d_{ls}^\dagger X_l^\dagger$ with $X_l = e^{-(g/\omega_0)(a_l^\dagger - a_l)}$. The relevant parameters of (1) become renormalized: $\tilde{E}_d = E_d - (g^2/\omega_0)$, $\tilde{U} = U - 2(g^2/\omega_0)$, $\tilde{V} = V X_l$ and $\tilde{t} = t X_1 X_2$. Factor X describes the effect of phonon cloud accompanying the tunneling. In the following we replace X_l by its expectation value $\langle X \rangle = e^{-(g/\omega_0)^2 (n_0 + 1/2)}$ [26]. The electron and phonon subsystems become decoupled. Holstein coupling lowers the energy of doubly occupied orbitals with respect to singly occupied or empty ones. It is convenient to rewrite the effective polaron Hamiltonian in the basis of bonding (-) and antibonding (+) orbital operators $d_{\nu s} = (1/\sqrt{2})(d_{1s} \pm d_{2s})$ ($\nu = \pm$). The effective electron (polaron) Hamiltonian then reads:

$$\begin{aligned} \tilde{H} = & \sum_{\nu s} (E_d \pm \tilde{t}) n_{\nu s} + \sum_{\nu} \frac{\tilde{U} + U'}{2} (n_{\nu\uparrow} n_{\nu\downarrow} + n_{\nu\uparrow} n_{\nu\downarrow}) \\ & + U' \sum_s n_{+s} n_{-s} + \frac{\tilde{U} - U'}{2} (C_{flip} - S_{flip}) \quad (3) \\ & + \sum_{k\alpha \nu s} E_{k\alpha \nu s} n_{k\alpha \nu s} + \sum_{k\alpha \nu s} \tilde{V} (c_{k\alpha \nu s}^\dagger d_{\nu s} + h.c.) \end{aligned}$$

The last term represents charge-flip $C_{flip} = T_+^+ T_-^- + h.c.$ and spin-flip $S_{flip} = S_+^+ S_-^- + h.c.$ processes, where spin and orbital isospin are given by the fermionic operators as follows:

$$\begin{aligned} S_\nu^Z &= (n_{\nu\uparrow} - n_{\nu\downarrow})/2 \\ S_\nu^- &= d_{\nu\downarrow}^\dagger d_{\nu\uparrow} = (S_\nu^+)^{\dagger} \quad (4) \end{aligned}$$

and

$$\begin{aligned} T_\nu^Z &= (n_\nu - 1)/2 \\ T_\nu^- &= d_{\nu\uparrow} d_{\nu\downarrow} = (T_\nu^+)^{\dagger}. \quad (5) \end{aligned}$$

To discuss correlations we use generalized finite - U slave boson mean field approximation (SBMFA) of Kotliar and Ruckenstein [27–29]. Compared to the more exact numerical approaches e.g. most powerful method - renormalization group approach (NRG) [30], SBMFA has narrower range of applicability. Whereas NRG can treat systems with a broad and continuous spectrum of energies for arbitrary temperatures, SBMFA is correct only in the unitary Kondo regime or close to it, but also leads to local Fermi-liquid behavior at zero temperature. It gives reliable results of linear conductance also for systems with weakly broken symmetry, as confirmed by experiments and NRG calculations [31, 32]. SBMFA breaks down at higher temperatures, but going beyond mean field by taking into account slave boson fluctuations would remove this deficiency. SBMFA

has higher computational efficiency than NRG and allows analysis of nonlinear transport. In the context of e-ph problem considered in the following, it is worth mentioning, that only a limited number of bosonic states can be taken into account in numerical diagonalization carried out within NRG and this imposes some restrictions on phonon frequencies and e-ph coupling strengths that may be considered in NRG procedure [30]. For analysis of correlation effects we introduce, in the spirit of SB approach, a set of boson operators for each electronic configuration of the system. The auxiliary bosons e, p, d, t, f project onto empty, single, double, triple and fully occupied states. The single occupation projectors $p_{\nu s}$ are labeled by orbital and spin numbers, the triple occupancy bosons $t_{\nu s}$ by orbital and spin of the hole and among d operators there are two classes d_ν which correspond to the occupation of the single orbital by two electrons ($\uparrow\downarrow, 0$), ($0, \uparrow\downarrow$) and four $d_{ss'}$ operators representing states (\uparrow, \uparrow), (\uparrow, \downarrow), (\downarrow, \uparrow), (\downarrow, \downarrow). In order to eliminate additional unphysical states introduced by SB representation one supplements SB Hamiltonian by conditions of charge conservation and completeness relations:

$$Q_{\nu s} = p_{\nu s}^\dagger p_{\nu s} + d_{ss}^\dagger d_{ss} + d_{\nu}^\dagger d_{\nu} + d_{s-s}^\dagger d_{s-s} + t_{\nu s}^\dagger t_{\nu s} + \sum_s t_{-\nu s}^\dagger t_{-\nu s} + f^\dagger f \quad (6)$$

and

$$I = e^\dagger e + \sum_{\nu s} p_{\nu s}^\dagger p_{\nu s} + \sum_{\nu} d_{\nu}^\dagger d_{\nu} + \sum_{\nu s} d_{ss'}^\dagger d_{ss'} + \sum_{\nu s} t_{\nu s}^\dagger t_{\nu s} + f^\dagger f. \quad (7)$$

The constraints are incorporated into (4) via the Lagrange multipliers λ and $\lambda_{\nu s}$. The corresponding K-R Hamiltonian then reads:

$$\begin{aligned} \tilde{H}^{sbMFA} &= \sum_{\nu s} (E_d \pm \tilde{t}) N_{\nu s}^f + U' \sum_s d_{ss}^\dagger d_{ss} + \\ &\frac{\tilde{U} + U'}{2} (d_{s\bar{s}}^\dagger d_{s\bar{s}} + \sum_{\nu} d_{\nu}^\dagger d_{\nu}) \\ &\frac{\tilde{U} - U'}{2} (d_{\nu}^\dagger d_{\bar{\nu}} - d_{s\bar{s}}^\dagger d_{s\bar{s}} + h.c.) \\ &+ \sum_{\nu s} (\tilde{U} + 2U') t_{\nu s}^\dagger t_{\nu s} + (2\tilde{U} + 4U') f^\dagger f + \\ &\sum_{\nu s} \lambda_{\nu s} (N_{\nu s} - Q_{\nu s}) + \lambda (I - 1) + \sum_{k\nu s} E_{k\nu s} n_{k\nu s} + \\ &\sum_{k\nu s} \tilde{V} (c_{k\nu s}^\dagger z_{\nu s} f_{\nu s} + h.c.) \end{aligned} \quad (8)$$

where $N_{\nu s}^f = f_{\nu s}^\dagger f_{\nu s}$ is the pseudofermion occupation number operator [27]. $z_{\nu s} = (e^\dagger p_{\nu s} + p_{\nu-s}^\dagger d_{\nu} + p_{-\nu s}^\dagger d_{ss} + p_{-\nu-s}^\dagger d_{s-s} + d_{s-s}^\dagger t_{-\nu-s} + d_{-\nu}^\dagger t_{\nu s} + d_{-ss}^\dagger t_{-\nu s} + t_{-\nu-s}^\dagger) / \sqrt{(1 - Q_{\nu s}) Q_{\nu s}}$ and $\lambda, \lambda_{\nu s}$ are the renormalization parameter and the Lagrange multipliers.

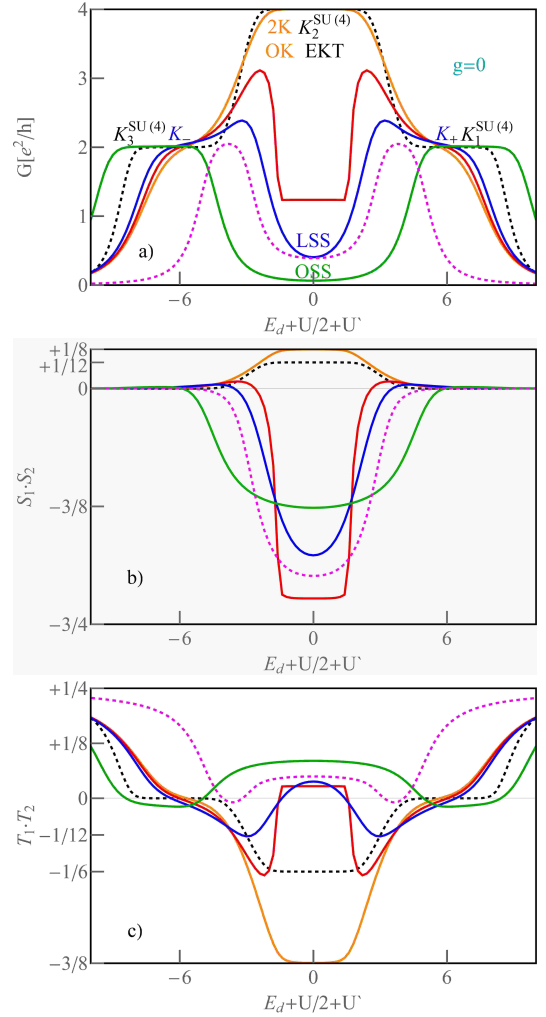


Figure 2. (Color online) a) Conductance G as a function of dot energy level E_d for $U = U' = 6$ ($t = 0$, black dashed line), $U = 6, U' = 5$ ($t = 0, 0.2, 0.4, 2$: orange, red, blue and green curves) and $U = 6, U' = 0$ ($t = 2$, magenta dashed line). b, c) Corresponding spin-spin $S_1 \cdot S_2$ and isospin-isospin $T_1 \cdot T_2$ correlators ($g = 0, \Gamma = 0.1$).

The characteristic temperatures are given by the width and the position of the quasiparticle resonances: $T^* = \min\{T_\nu^*\} = \sqrt{(E_d \pm \tilde{t} + \lambda_{\nu s})^2 + (\tilde{\Gamma}|z_{\nu s}|^2)^2}$. For the case of Kondo resonance $T^* = T_K$. In the MFA the slave boson operators are replaced by their expectation values and the stable solutions are found from the saddle point of partition function i.e. from the minimum of the free energy with respect to the mean values of slave bosons and Lagrange multipliers. SBMFA best describes spin and orbital fluctuations in the unitary Kondo regime. For low temperatures $T < T_K$, and low voltages $eV < kT_K$ MFA's neglect of bosonic field fluctuations and renormalized level fluctuations is justified, and this is the regime we limit ourselves to in this article. Due to separability of electron and phonon degrees of freedom, which results from L-F transformation, the dot Green's functions have

Table I. Dominant slave bosons, charge fluctuations on local dot orbitals and molecular DQD orbitals, spin-spin and isospin-isospin correlators and conductance for the discussed quantum phases.

	SB amplitudes	$\Delta N_{1,2}^2$	ΔN_{\pm}^2	$\langle S_1 \cdot S_2 \rangle$	$\langle T_1 \cdot T_2 \rangle$	$G[e^2/h]$
$K_2^{SU(4)}$	$d_{\pm}^2 = d_{ss'}^2 = 1/6$	0	1/3	0	-1/12	4
$K_{1,3}^{SU(4)}$	$p_{\nu s}^2 = 1/4, t_{\nu s}^2 = 1/4$	0	1/4	0	0	2
EKT	$d_{ss'}^2 = 1/4$	1/4	1/3	$0 + 1/12 = +1/12$	$0 - 1/6 = -1/6$	4
$2K$	$d_{ss'}^2 = 1/4$	1/2	0	$0 + 1/8 = +1/8$	$-1/4 - 1/8 = -3/8$	4
K_{\pm}	$p_{\nu s}^2 = 1/2, t_{\nu s}^2 = 1/2$	1/4	0	0	0	2
LSS	$d_{-}^2 \approx 1$	0	1	$-1/2 - 1/4 = -3/4$	0	0
SOK	$d_{\pm}^2 = 1/2$	0	1	$-1/2 - 1/4 = -3/4$	0	4
OSS	$d_{-}^2 = 1$	1/2	0	$-1/4 - 1/8 = -3/8$	$1/4 - 1/8 = +1/8$	0
COK	$e^2 = f^2 = d_{\pm}^2 = 1/4$	1	1	0	$0 + 1/4 = +1/4$	4
IOK	$d_{\pm}^2 = 1/2$	1	1	0	$1/2 - 1/4 = +1/4$	4

the form:

$$G_{\nu s}(t) = -i\theta(t)(\langle d_{\nu s}(t)d_{\nu s}^{\dagger}(0) \rangle \langle X(t)X^{\dagger}(0) \rangle + \langle d_{\nu s}^{\dagger}(0)d_{\nu s}(t) \rangle \langle X^{\dagger}(0)X(t) \rangle) \quad (9)$$

with $\langle X(t)X^{\dagger}(0) \rangle = e^{-\theta(t)}$, where $\theta(t) = (g/\omega)^2[n_0(1 - e^{i\omega_0 t}) + (n_0 + 1)(1 - e^{-i\omega_0 t})]$. For $T = 0$ $\langle X^{\dagger}(0)X(0) \rangle$ is reduced to $\sum_{n=0}^{+\infty} L_n e^{i\omega_0 t}$, where $L_n = (1/n!)(g/\omega_0)^{2n} e^{-(g/\omega_0)^2}$. The Fourier transforms of the retarded electron Green's functions of the orbitals to which the phonons are attached is given by:

$$G_{\nu s}^R = \sum_n L_n [(1 - f(E - n\omega_0))\tilde{G}_{\nu s}^R(E - n\omega_0) + f(E + n\omega_0)\tilde{G}_{\nu s}^R(E + n\omega_0)], \quad (10)$$

where $f(E)$ is a Fermi function and \tilde{G} are the Green's functions determined with the use of Hamiltonian (3). The linear conductances are given by a Landauer-type formula:

$$G = G_+ + G_- = (2e^2/h) \sum_{\nu} \sin[\pi N_{\nu}] = (2e^2/h) \sum_{\nu} T_{\nu}(0). \quad (11)$$

Here, transmissions are defined as:

$$T_{\nu}(E) = \sum_{n=-\infty}^{+\infty} \frac{\tilde{\Gamma}|z_{\nu s}|^2 L_n}{E + n\omega_0 - (\tilde{E}_d \pm \tilde{t} + \lambda_{\nu s}) + i\tilde{\Gamma}|z_{\nu s}|^2} \quad (12)$$

The spin-spin and isospin-isospin correlation operators expressed by fermion operators are given by [13]:

$$S_1 \cdot S_2 = (1/4) \left(\sum_{ss'} n_{1s} n_{2s'} - 2d_{1\downarrow}^{\dagger} d_{2\downarrow} d_{2\uparrow}^{\dagger} d_{1\uparrow} - 2d_{1\uparrow}^{\dagger} d_{2\uparrow} d_{2\downarrow}^{\dagger} d_{1\downarrow} \right) \quad (13)$$

and

$$T_1 \cdot T_2 = (1/4) \left(1 - \sum_{ls} n_{ls} + \sum_{ss'} n_{1s} n_{2s'} + 2d_{1\downarrow}^{\dagger} d_{2\downarrow} d_{1\uparrow}^{\dagger} d_{2\uparrow} + 2d_{1\downarrow}^{\dagger} d_{2\downarrow} d_{1\downarrow}^{\dagger} d_{2\uparrow} \right). \quad (14)$$

The orbital (charge) fluctuations read $\Delta N_{l(\nu)}^2 = (Q_{l(\nu)} - N_{l(\nu)})^2$.

III. RESULTS AND DISCUSSION

In the following we discuss modifications of many-body effects in parallel double dot systems caused by electron-phonon coupling. The calculations were performed in the strong correlation regime assuming Coulomb parameter $U = 6$, coupling to the leads $\Gamma = 0.1$, phonon energies $\omega_0 = 1/8$ and electron - phonon coupling strength g in the range 0.01 – 0.8. All numerical results are presented in the relative energy units choosing $D/50$ as the unit.

As an introduction to the description of variety of many-body states occurring in the considered system let us first discuss the reference case of the dots in the absence of phonons and concentrate on the role of interdot hopping t . Fig 2a compares conductances of DQD for different values of t . The dotted black line for $t = 0$ and $U = U'$ illustrates the well-known SU(4) Kondo case with plateaus of $2e^2/h$ and $4e^2/h$ for $n = 1, 3$ and $n = 2$ respectively. Dotted magenta curve presents conductance for $U' = 0$ and finite $t = 2$ with conductance for $n = 2$ strongly reduced compared to the unitary limit. In this range Kondo resonance destruction occurs. Other curves correspond to the cases of different intra and interdot Coulomb interactions ($U = 6$, $U' = 5$) and finite t . The charge stability regions narrow and consequently plateaus for $n = 1$ and $n = 3$ are replaced by functions increasing towards the e-h symmetry point. For very small values of t many-body state forms with effective fluctuating spin and orbital pseudospin ($p_{\pm s}^2 = 1/4$), which we call $K_1^{SU(4)}$ and is in fact slightly broken SU(4) Kondo state (see Table 1). With increasing t state $K_{1,3}^{SU(4)}$ transforms into SU(2) spin Kondo states (K_{\pm}) on bonding ($n = 1$) or antibonding ($n = 3$) orbitals respectively with only slight change in conductance, but drastic change in Kondo temperature (inset of Fig.3a). For $n = 2$ the effect of increase of

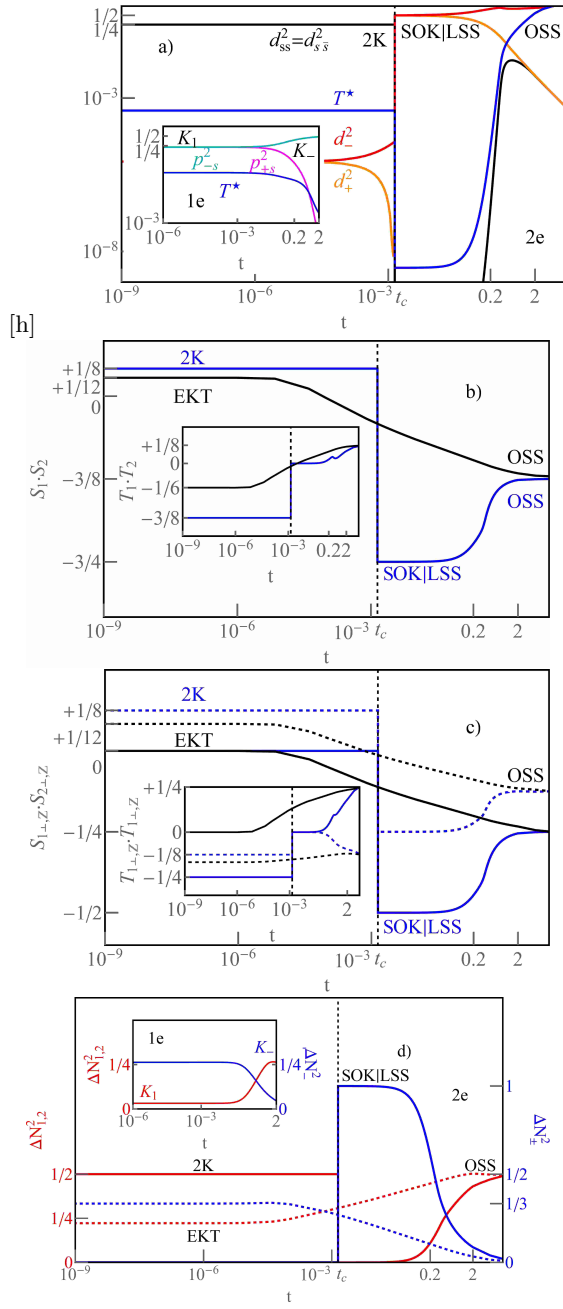


Figure 3. (Color online) a) Slave boson amplitudes and characteristic temperature T^* (blue line) ($U = 6, U' = 5$) for $2e$ and in $1e$ regime (inset). b) Total correlators $S_1 S_2$ and $T_1 T_2$ (inset) for $U = U' = 6$ (black curves) and $U = 6U' = 5$ (blue lines). c) Transversal (\perp , solid lines) and longitudinal (\parallel) parts of spin-spin and isospin-isospin correlators for $U = U' = 6$ (black curves) and $U = 6U' = 5$ (blue lines). d) Orbital ΔN_{\pm}^2 and dot $\Delta N_{1,2}^2$ fluctuations for $2e$ region (solid and dashed lines are for $U = U' = 6$ and $U = 6, U' = 5$ respectively) and charge fluctuations for $1e$ (inset).

t is more decisive, because this not only makes the description in the language of molecular orbitals more appropriate for large t , but also introduces spin and isospin

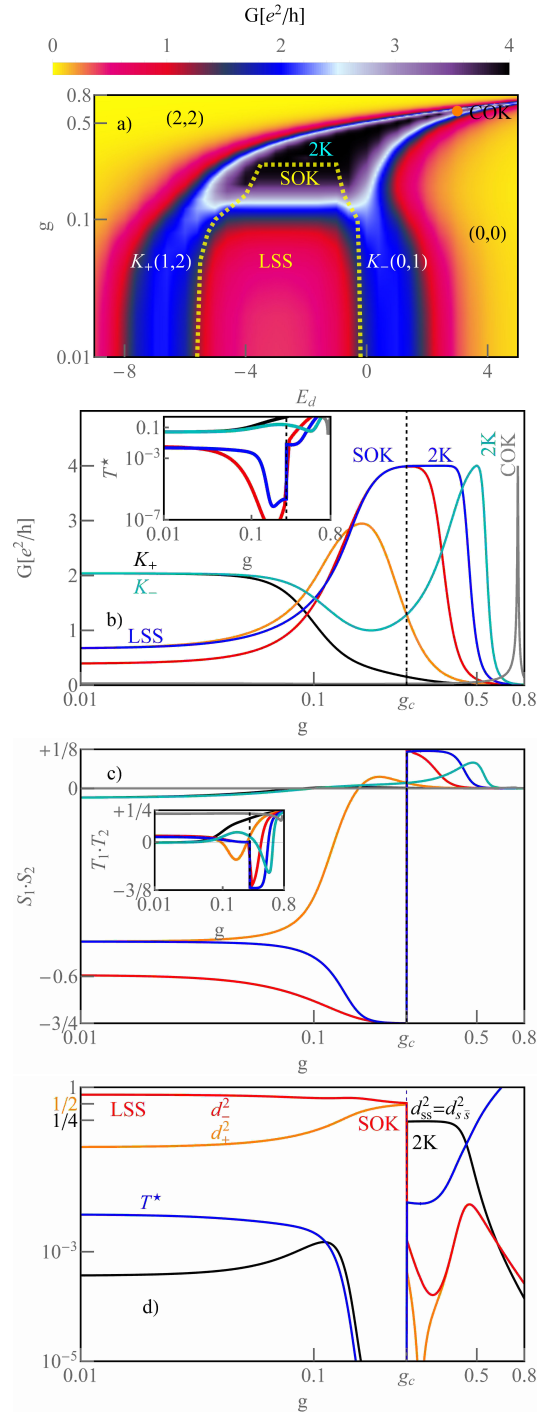


Figure 4. (Color online) a) Conductance map vs. dot energy level and phonon-coupling strength g with marked quantum phases (see Tab.1, $g > 0, U = 6, U' = 0, t = 2, \omega_0 = 1/8$ and $\Gamma = 0.1$). Dashed yellow line separates the ground states of LSS and OK phases from the others in $2e$ range. Orange dot symbolizes the point $U = 0$. b) Cross sections of G for $E_d = -7, -5, -3, -1, 1, 6$ (black, orange, red, blue, cyan and gray). Inset presents the corresponding characteristic temperatures. c) Spin-spin and isospin-isospin (inset) correlators. d) Dominating slave-boson amplitudes and T^* for $E_d = -1$ presented on border of the Kondo like quantum phases SOK and $2K$.

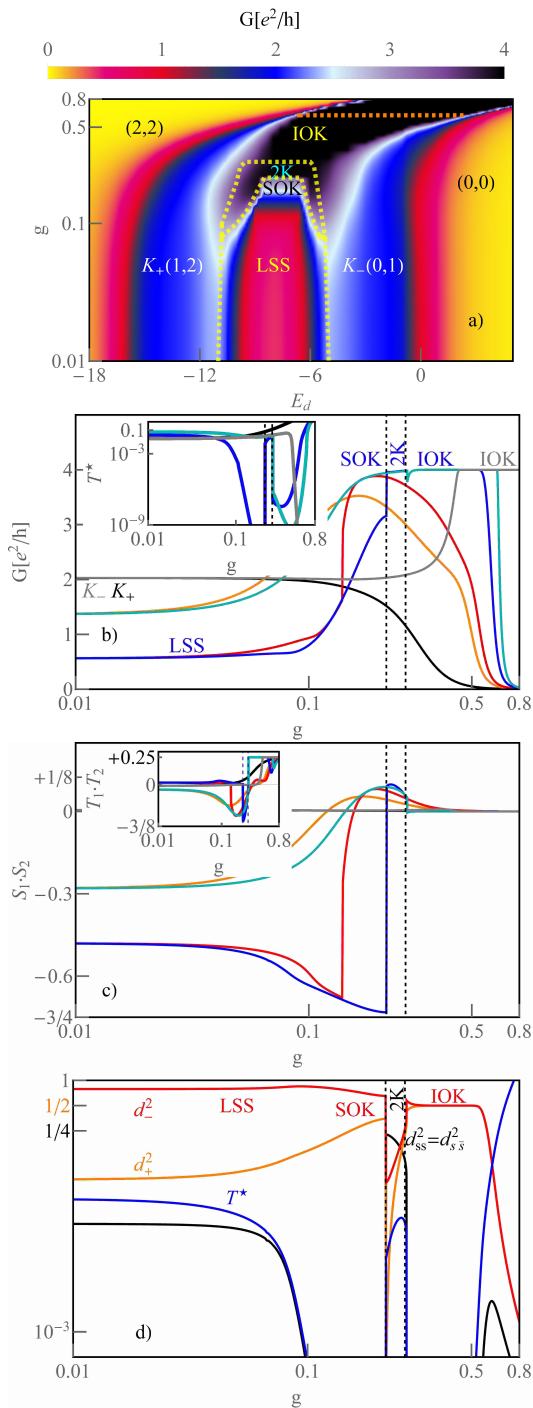


Figure 5. (Color online) a) Conductance map vs. dot energy level and phonon-coupling strength g with marked quantum phases ($g > 0, U = 6, U' = 5, t = 0.4, \omega_0 = 1/8$ and $\Gamma = 0.1$). Dashed yellow line separates the ground states of LSS, SOK and 2K phases from the others in 2e range. Orange dashed line symbolizes the line where $U = 0$. b) Cross sections of G for $E_d = -14, -10, -9, -7, -6, -2$ (black, orange, red, blue, cyan and gray). Inset presents the corresponding characteristic temperatures. c) Spin-spin and isospin-isospin (inset) correlators. d) Dominating slave-boson amplitudes and T^* for $E_d = -1$.

correlations. For $t = 0$, or very small values of interdot hopping the spin-orbital Kondo effect (2K) occurs, where in contrast to $SU(4)$ effect for $n = 2$, not all six states fluctuate, but only four of them ($d_{ss'}^2 = 1/4$, Tab. 1). Already for $t = 0$ spin and isospin correlations are non-zero ($\langle S_1 \cdot S_2 \rangle = +1/8$, $\langle T_1 \cdot T_2 \rangle = -3/8$, Fig. 3b). For the critical value of interdot hopping $t_c \sim 1.4 \cdot 10^{-3}$ sharp transition into orbital (charge) spin correlated Kondo state SOK ($\langle S_1 \cdot S_2 \rangle \sim -3/4$) occurs, where cotunneling induced fluctuations between two-electron states characterized by double occupancy of one of the dots and vacancy of the second take place $(0, 2) \leftrightarrow (2, 0)$ and $G \cong 4$. The isospin is screened $\langle T_1 \rangle = 0$. Increase of tunnel coupling causes the suppression of conductance. Kondo temperature is drastically reduced. For still larger interdot tunneling Kondo resonance is destroyed and bonding state becomes favorable. Local spin singlet (LSS) forms in this case with antiparallel spin correlations and vanishing isospin correlations. In this case, the description in the language of the local orbitals on the dots is useful. $\langle S_1 \cdot S_2 \rangle$ preserves a value close to $-3/4$. Charge fluctuations associated with the local states of the dots are negligible, those associated with the molecular states are of course finite (Fig.3d, Tab.1). Increasing hopping further results in a smooth transition to orbital spin singlet state (OSS) with weaker spin correlations than in LSS state, but also negative. Both longitudinal and transverse contributions are twice reduced in comparison to LSS (Tab.1). Isospin correlator of the bonding state in OSS state $\langle T_1 \cdot T_2 \rangle = 1/4 - 1/8 = +1/8$ with opposite signs of longitudinal and transverse contributions. Fig. 3b compares the dependencies of the correlation function on the value of the hopping integral for $U' = 5$ with the analogous dependencies for $U = U' = 6$. In the former case transition at t_c is sharp, whereas for the latter it is smooth. Ground states below t_c for $U' = 5$ and $U = U' = 6$ are double Kondo phase (2K) and enhanced Kondo temperature phase (EKT) respectively. Both these states are characterized by the same slave boson occupations ($d_{ss'}^2 = 1/4$), Tab. 1), the same unitary conductances $G = 4e^2/h$, but charge fluctuations and spin and isospin correlations functions are different (Tab.1 and Fig. 3b,c). Description of 2K state in the language of effective fluctuations between molecular states is appropriate, whereas for EKT both local and molecular picture play similar, less relevant role. Fig. 3d shows gate dependencies of local charge fluctuations at the dots (ΔN_l^2) and charge fluctuations on the molecular dot orbital (ΔN_ν^2) for $n = 2$ and $n = 1$ (inset). If orbital occupancy fluctuations ΔN_ν^2 are smaller than local occupancy fluctuations ΔN_l^2 then orbital picture is adequate. As it seen from Fig. 3b below t_c $\langle S_1 \cdot S_2 \rangle > 0$, and for $t > t_c$ $\langle S_1 \cdot S_2 \rangle < 0$, i.e. antiparallel spin correlations develop. Fig. 3c presents longitudinal and transverse contributions to the spin and isospin correlation functions for different two-electron ground states of DQD.

To discuss the impact of phonons on the ground-state

phase diagrams we choose $t = 2$ for illustration of the case of electrostatically decoupled dots ($U' = 0$) and $t = 0.4$ for the capacitive coupling $U' = 5$. With this choice for $g = 0$ in both cases, magnetic ground state LSS occurs in double occupancy region. Fig. 4a shows conductance vs. dot energy and e-ph coupling constant for $U' = 0$. The numbers in brackets denote occupancies of molecular orbitals, N_- for bonding orbital and N_+ for antibonding. Fig. 4b presents selected, representative cross-sections of the conductance map for the fixed unperturbed energies of the dots. i.e. dependencies of conductance on e-ph coupling strength for different gate voltages, which for $g = 0$ correspond to occupations $n = 0, 1, 2, 3$ respectively. The spin Kondo state on antibonding orbital K_+ for $n = 3$ with $G \cong 2$ survives until relatively strong e-ph coupling strength (g), for still larger coupling the dots will be fully occupied (state $(2, 2)$, $n = 4$). For $n = 2$ and assumed value $t = 2$ the slightly perturbed LSS state ($d_{ss}^2 \sim 1$), characterized by low conductance and antiferromagnetic correlations occurs for weak coupling. This state evolves with increasing g towards orbital (charge) spin correlated Kondo state SOK. For $g = g_c$ a sharp transition into Kondo 2K state occurs with effective fluctuations between the four spin-orbitals ($d_{ss'}^2 = 1/4$, $G \cong 4$). In 2K state interdot spin correlations are positive ($\langle S_1 \cdot S_2 \rangle \sim +1/8$) and Kondo temperature is much higher than for SOK state. The above described transitions from LSS state into SOK and 2K are phonon induced. The spin Kondo state on bonding orbital K_- ($n = 1$) is suppressed with the increase of e-ph coupling. The dots becomes unoccupied ($n \cong 0$). For still stronger coupling, however, DQD becomes doubly populated ($n \cong 2$) and double Kondo state 2K is observed. It is seen from the conductance map (Fig. 4a), that some states from region $n = 1$ develop a bit differently. Increase of g results in a change of occupation $n = 1 \rightarrow n = 2$ and a direct transition from K_- into 2K occurs. It is realized for example for $E_d = 0.5$. We do not draw the cross-section for this case. Similar transitions accompany the change of occupation $n = 0 \rightarrow n = 2$ for $E_d < +3$. The grey curve on Fig. 4b ($E_d = 6$) corresponds to transition from empty state for weak and intermediate e-ph coupling into charge-orbital Kondo state (COK) ($G \cong 4$), where simultaneous effective fluctuations occur between empty and fully occupied states and between molecular orbitals ($e^2 = f^2 = d_{\pm}^2 = 1/4$). This is again example of phonon induced Kondo effect. COK forms for g so large that intrasite interaction becomes attractive ($U < 0$). This favors fluctuation of pairs of electrons or holes ($e \leftrightarrow f$). For extremely large e-ph coupling the dots are completely filled $(2, 2)$ due to the phonon induced attracting potential.

Now let us look, how the ground state picture is modified in the presence of capacitive interdot coupling (Fig.5). Qualitatively, the transitions in areas $n = 1$ and $n = 3$ do not differ significantly from those discussed for the case $U' = 0$. For $n = 2$ the LSS ground state occurring in the weak e-ph coupling range is, similarly to

the earlier discussed problem for $U' = 0$, first replaced by SOK state and for still higher values of g by 2K. For $g > 0.26$ however, the new many-body state appears: perturbed orbital Kondo effect, which we call isospin correlated Kondo effect (IOK, $\langle T_1 \cdot T_2 \rangle = +1/4$). This state can also be reached for strong e-ph coupling starting at $g = 0$ from the regions $n = 0$ or $n = 1$.

IV. SUMMARY AND CONCLUSIONS

Summarizing, in the present paper, we examined an impact of electron-phonon coupling on electron correlations in double dot system in parallel geometry with capacitive and tunnel coupling. In the spirit of Holstein's picture, it was assumed that phonons located on a given dot interact only with electrons on the same dot. Our analysis is addressed to molecular systems, where a strong coupling of local vibrations with electrons is expected, and to suspended quantum dots based on semiconductors, which can also be strongly influenced by phonons. Phonon-induced suppression of charging energies shifts and modifies the Coulomb blockade borders and narrows Coulomb valleys. The interplay of weakening of both Coulomb site energies and effective dot-lead coupling together with the changes in the separations of eigenenergies of DQD, due to phonon induced weakening of interdot hopping, affects various electronic correlations leading to the richness of emerging phenomena. Phonons remove or restore degeneracies destroying or reviving Kondo-like states engaging spin, orbital degrees of freedom or both of them. Competition of intersite spin or orbital correlation with local Kondo screening is also strongly influenced by vibrations. Besides various Kondo effects: spin, orbital, spin-orbital and charge-orbital resonances, forming due to participation of phonons, also local spin singlets with antiferromagnetic correlations appear in DQD coupled to local phonons. When attraction caused by phonons exceeds site Coulomb repulsion then cotunneling processes induce effective fluctuations of pairs of electrons or holes, which together with effective orbital fluctuations lead to charge-orbital Kondo effect.

The issues analyzed in this work concern elastic features of spectral densities which are reflected in the linear conductance. As far as we know, all experimental works on the Kondo effect with the participation of phonons concern inelastic effects. For verifications of our predictions on phonon induced modifications of Kondo ground state, experimental analysis of linear transport for different frequencies and different values of the e-ph coupling strength would be necessary. Detailed transport measurements for various phonon frequencies and different e-ph coupling strength are within the reach of the present technology both for semiconducting QDs embedded in a freestanding membrane and for carbon nanotubes [22–24].

-
- [1] G. Burkard, H.-A. Engel, and D. Loss, Spintronics and quantum dots for quantum computing and quantum communication, *Fortschr. Phys.* **48**, 965 (2000).
- [2] D. Awschalom, D. Loss, and N. Samarth, eds., *Semiconductor spintronics and quantum computation* (Springer, Berlin, Germany, 2002).
- [3] R. López, R. Aguado, and G. Platero, Nonequilibrium transport through double quantum dots: Kondo effect versus antiferromagnetic coupling, *Phys. Rev. Lett.* **89**, 136802 (2002).
- [4] J. C. Chen, A. M. Chang, and M. R. Melloch, Transition between quantum states in a parallel-coupled double quantum dot, *Phys. Rev. Lett.* **92**, 176801 (2004).
- [5] C. A. Büsser, A. E. Feiguin, and G. B. Martins, Electrostatic control over polarized currents through the spin-orbital Kondo effect, *Phys. Rev. B* **85**, 241310 (2012).
- [6] C. A. Büsser and G. B. Martins, Numerical results indicate a half-filling SU(4) Kondo state in carbon nanotubes, *Phys. Rev. B* **75**, 045406 (2007).
- [7] M.-S. Choi, R. López, and R. Aguado, SU(4) Kondo effect in carbon nanotubes, *Phys. Rev. Lett.* **95**, 067204 (2005).
- [8] E. Vernek, C. A. Büsser, E. V. Anda, A. E. Feiguin, and G. B. Martins, Spin filtering in a double quantum dot device: Numerical renormalization group study of the internal structure of the Kondo state, *Appl. Phys. Lett.* **104**, 132401 (2014).
- [9] D. Krychowski and S. Lipiński, Spin-orbital and spin Kondo effects in parallel coupled quantum dots, *Phys. Rev. B* **93**, 075416 (2016).
- [10] A. J. Keller, S. Amasha, I. Weymann, C. P. Moca, I. G. Rau, J. A. Katine, H. Shtrikman, G. Zaránd, and D. Goldhaber-Gordon, Emergent SU(4) Kondo physics in a spin-charge-entangled double quantum dot, *Nat. Phys.* **10**, 145 (2014).
- [11] R. Leturcq, C. Stampfer, K. Inderbitzin, L. Durrer, C. Hierold, E. Mariani, M. G. Schultz, F. von Oppen, and K. Ensslin, Franck-Condon blockade in suspended carbon nanotube quantum dots, *Nat. Phys.* **5**, 1745 (2009).
- [12] E. M. Höhberger, T. Krämer, W. Wegscheider, and R. H. Blick, In situ control of electron gas dimensionality in freely suspended semiconductor membranes, *Appl. Phys. Lett.* **82**, 4160 (2003).
- [13] J. Mravlje and A. Ramšak, Kondo effect and channel mixing in oscillating molecules, *Phys. Rev. B* **78**, 235416 (2008).
- [14] P. Florków and S. Lipiński, Impact of electron-phonon coupling on electron transport through T-shaped arrangements of quantum dots in the Kondo regime, *Beilstein J. Nanotechnol.* **12**, 1209 (2021).
- [15] P. S. Cornaglia, D. R. Grempel, and H. Ness, Quantum transport through a deformable molecular transistor, *Phys. Rev. B* **71**, 075320 (2005).
- [16] W. Rudziński, Phonon-assisted spin-polarized tunneling through an interacting quantum dot, *Journal of Physics: Condensed Matter* **20**, 275214 (2008).
- [17] C. Wang, J. Ren, B. W. Li, and Q. H. Chen, Quantum transport of double quantum dots coupled to an oscillator in arbitrary strong coupling regime, *Eur. Phys. J. B* **85**, 110 (2012).
- [18] M. D. Nuñez Regueiro, P. S. Cornaglia, G. Usaj, and C. A. Balseiro, Slave boson theory for transport through magnetic molecules with vibronic states, *Phys. Rev. B* **76**, 075425 (2007).
- [19] K. Bocian and W. Rudziński, Phonon-assisted Andreev reflection in a hybrid junction based on a quantum dot, *Eur. Phys. J. B* **88**, 50 (2015).
- [20] D. Rakhmilevitch, R. Korytár, A. Bagrets, F. Evers, and O. Tal, Electron-vibration interaction in the presence of a switchable Kondo resonance realized in a molecular junction, *Phys. Rev. Lett.* **113**, 236603 (2014).
- [21] E. M. Weig, R. H. Blick, T. Brandes, J. Kirschbaum, W. Wegscheider, M. Bichler, and J. P. Kotthaus, Single-electron-phonon interaction in a suspended quantum dot phonon cavity, *Phys. Rev. Lett.* **92**, 046804 (2004).
- [22] D. M.-T. Kuo and Y. C. Chang, Tunneling current through a quantum dot with strong electron-phonon interaction, *Phys. Rev. B* **66**, 085311 (2002).
- [23] V. N. Popov and P. Lambin, Radius and chirality dependence of the radial breathing mode and the g -band phonon modes of single-walled carbon nanotubes, *Phys. Rev. B* **73**, 085407 (2006).
- [24] E. Mariani and F. von Oppen, Electron-vibron coupling in suspended carbon nanotube quantum dots, *Phys. Rev. B* **80**, 155411 (2009).
- [25] I. G. Lang and Y. A. Frisov, Kinetic theory of semiconductors with low mobility, *Sov. Phys. JEPT* **16**, 1301 (1963).
- [26] G. D. Mahan, *Many-Particle Physics* (Springer New York, NY, 2000).
- [27] G. Kotliar and A. E. Ruckenstein, New functional integral approach to strongly correlated Fermi systems: The Gutzwiller approximation as a saddle point, *Phys. Rev. Lett.* **57**, 1362 (1986).
- [28] B. Dong and X. L. Lei, Kondo-type transport through a quantum dot: a new finite-U slave-boson mean-field approach, *J. Phys.: Condens. Mat.* **13**, 9245 (2001).
- [29] D. Krychowski and S. Lipiński, Intra- and inter-shell Kondo effects in carbon nanotube quantum dots, *Eur. Phys. J. B* **91**, 8 (2018).
- [30] R. Bulla, T. A. Costi, and T. Pruschke, Numerical renormalization group method for quantum impurity systems, *Rev. Mod. Phys.* **80**, 395 (2008).
- [31] D. Mantelli, C. Paşcu Moca, G. Zaránd, and M. Grifoni, Kondo effect in a carbon nanotube with spin-orbit interaction and valley mixing: A DM-NRG study, *Phys. E: Low-Dimens. Syst. and Nanostructures* **77**, 180 (2016).
- [32] B. M. de Souza Melo, L. G. G. V. D. da Silva, A. R. Rocha, and C. Lewenkopf, Quantitative comparison of Anderson impurity solvers applied to transport in quantum dots, *J. Phys.: Condens. Mat.* **32**, 095602 (2019).